JOURNAL OF AIRCRAFT
Vol. 42, No. 6, November–December 2005

Limit-Cycle Oscillation Flight-Test Results for Asymmetric Store Configurations

Kenneth S. Dawson* and Daniel L. Maxwell†
TYBRIN Corporation, Eglin Air Force Base, Florida 32542-6865

A conventional approach for flutter certification of asymmetric external store configurations on fighter aircraft is to analyze each side of the aircraft using half-span models. The flutter speed for the asymmetric configuration is then assumed to be no less than the flutter speed of either half-span solution. Recent certification efforts on the F-16 have involved asymmetrically carried stores that were previously certified for symmetric carriage. For the present work, asymmetric F-16 external store configurations were studied to investigate their aeroelastic behavior and relationship to similar symmetrically loaded external store configurations. Linear flutter analyses utilizing full-span finite element and aerodynamic models were used to predict the flutter boundaries of the asymmetric external store configurations. It was found that solutions using full-span models predicted lower flutter speeds in some cases for an asymmetric configuration than the comparable flutter speeds using the half-span model. The mode shapes of the asymmetric configuration indicate coupling mechanisms on at least one wing are similar to the symmetric configurations; however, they are unique in that the frequencies of these modes have shifted. Flutter flight tests on the F-16 were performed to validate the analytical results. The test results from the asymmetrically loaded configurations were compared to the test results for similar symmetrically loaded configurations. The oscillatory response behavior of the asymmetric configurations is shown to be primarily antisymmetric. Also, the flight-test results show limit-cycle oscillation behavior that correlates to the full-span linear flutter analysis. Specifically, it is shown that two flutter sensitive half-span configurations can be combined into one asymmetric configuration that exhibits no aeroelastic instabilities in flight. Conversely, it is shown that two aeroelastically stable, half-span configurations can be combined asymmetrically, which results in a configuration with lower, aeroelastically critical flutter speeds. These cases demonstrate the need for flutter analyses of the full aircraft structure for certification of asymmetric external store configurations.

Introduction

TRANSONIC flutter and limit-cycle oscillations (LCO) are of significant interest for several fighter aircraft, primarily those with external store configurations. Bunton and Denegri[1] elaborate on the impact of LCO and its relationship to classical flutter. It is generally accepted that LCO is the response caused by the nonlinear interaction of the structural and aerodynamic forces acting on the wing structure. Cunningham and Meijer[2,3] have shown that shock-induced trailing-edge separation resulting in nonlinear aerodynamic forces has a significant effect on the LCO mechanism. Assuming a different approach, Chen et al.[4] showed that nonlinear structural damping was a significant contributory factor to LCO. Although this research was performed in an attempt to predict LCO onset and amplitude levels, Denegri[5] contends that linear flutter analyses are adequate to identify the oscillation frequency and modal composition of the LCO mechanism. This paper examines the effectiveness of using linear analyses to predict aeroelastic instabilities for asymmetric external store configurations on the F-16. Also examined is the conventional industry practice that half-span finite element and aerodynamic models are sufficient to provide flutter certification and airspeed limits for asymmetric configurations.

Presented as Paper 2003-1427 at the AIAA/ASME/ASCE/AHS/ASC 44th Structures, Structural Dynamics, and Materials Conference, Norfolk, VA, 7–10 April 2003; received 12 May 2004; revision received 2 February 2005; accepted for publication 14 February 2005.

*Principal Flutter Engineer, U.S. Air Force SEEK EAGLE Office, 205 West D Avenue, Suite 348. Senior Member AIAA.

†Senior Flutter Engineer, U.S. Air Force SEEK EAGLE Office, 205 West D Avenue, Suite 348. Member AIAA.

Recent F-16 flight-test results have exhibited the classifications of typical and nontypical LCO as defined by Denegri in Ref. 5, although the configurations had asymmetrically loaded external stores. Linear analyses of asymmetric store configurations requiring certification have historically been absent because of the increased complexity and time requirements. The certification of symmetric store loadings has typically involved performing flutter analyses using half-span finite element and aerodynamic models with symmetric and antisymmetric boundary conditions. The download of a store with the half-span model assumes side-to-side symmetry, and it is typically assumed that any flutter criticality will be less severe with one or more stores absent as a result of the asymmetry. Katz[6] examined the effect of asymmetry caused by mass and stiffness variations at one location on a fighter aircraft wing. This study concluded that the effect of the asymmetry would only increase flutter speeds. Katz also expounded the standard assumption concerning asymmetric configurations resulting from the download of a single store from a symmetrically loaded configuration. For example, assume that an aircraft carries configuration X on one side and configuration Y on the other. It would then be assumed that the flutter speeds for this combination XY would be no lower than the lowest flutter speeds of either symmetric configuration XX or YY. Sensburg et al.[7] and Lotze[8] have shown that flutter speeds for asymmetric configurations could either be higher or lower than the flutter speeds of either symmetric half, although the change found in the flutter speeds could be attributed to a change in the coupling modes from store pitch and wing bending to store pitch and store roll. Flutter solution techniques presented by Lotze and by Maricic[9] still assumed a half-span model approach incorporating the asymmetric modes with the symmetric and antisymmetric modes. Guruswamy and Tu[10] used a full-span model to show lower analytical flutter speeds for a clean wing configuration with asymmetric modes when compared to the same wing with only purely symmetrical and antisymmetrical modes.

Flutter flight tests[11] of the F-16 and linear flutter analyses using a full-span finite element model (FEM) have shown that an asymmetric configuration can produce lower flutter speeds than the symmetrically loaded configurations corresponding to either

wing. The flight-test results presented here are grouped into two sets. Set I shows two aeroelastically stable, symmetrically loaded configurations. The asymmetric combination of these two configurations results in low analytical flutter crossings that are confirmed in the flight test as LCO. Set II shows two symmetrically loaded configurations with low analytical flutter crossings exhibiting LCO in flight. The asymmetric combination of these two configurations shows high analytical flutter speeds, and no aeroelastic instability is detected in flight. Analyses and mode shapes are examined to determine if the resulting lower asymmetric flutter speeds are simply different modes coupling, or if the mass asymmetry results in a unique asymmetric flutter mode.

Asymmetric Configurations

One of the most restrictive problems in external store certification is the tremendous volume of flutter analysis cases that must be examined in order to provide airspeed limits for a given store carriage configuration and all of its store download permutations. The number of store download permutations increases exponentially as each additional external station is included in the analytical solution. A full-span finite element model including asymmetric mass or stiffness conditions is further complicated by the fact that F-16 pylons with differing mass properties are interchangeable at four different locations. From a structural dynamics perspective, different external store configurations essentially alter the mass and rotational inertia characteristics of the wing structure. If different weapon carriage pylons are involved, then the aeroelastic stiffness characteristics are altered as well. The presence of stores and pylons can also significantly affect the aerodynamics. In addition, multiple stores can be carried and downloaded on a typical fighter aircraft. When all of these factors are taken into consideration, it becomes clear that a tremendous number of aeroelastic systems exist for each store carriage configuration.

Historically, typical certification requests for the F-16 were for symmetrically loaded external store configurations. Recent certification requests of external store configurations typically include at least two store asymmetries. Thus, enormous quantities of flutter analyses must be performed for a single aircraft weapon configuration. Typical F-16 flutter analysis utilizing a half-span model that examines all downloads but considers only symmetric external store configurations requires 80 solutions for a given altitude and Mach number, 40 each for symmetric and antisymmetric boundary conditions incorporating five distinct fuel conditions. A complete examination of all store downloads and pylon variations for an asymmetric F-16 configuration might require more than 3000 distinct flutter solutions. The complexity of running full-span analyses and the even more time-consuming task of interpreting these results led to the question of whether or not certification of asymmetric configurations could be safely and effectively deduced from half-span analyses and the multitude of flight-test data that exists for various symmetrically loaded configurations.

Flight-Test Results

Flight-test results are shown for the six external store configurations described in Table 1. In the table, "Lau" represents an empty missile rail launcher, and "FFF", "FEF", "FEE", and "EEE" represents various fuel states from full to empty for the external fuel tanks. Set I involves asymmetrically loaded configuration 1, which is the combination of the symmetrically loaded configurations 2 and 3. This set shows two symmetrically loaded configurations free from aeroelastic concerns, including LCO; however, combining the two different wings into one asymmetric configuration results in a significantly lower flutter crossing, as demonstrated by LCO encountered during the flight test. Set II involves asymmetrically loaded configuration 4, which is the combination of the symmetrically loaded configurations 5 and 6. This case shows two symmetric loadings that have a flutter mechanism resulting in LCO and the asymmetric combination of the two that does not.

Configurations 1 and 3 of set I and configurations 4 through 6 of set II were flown on the same block 25 F-16. Configuration 2 of set I was flown on a block 40 F-16 aircraft. The block 40 F-16 incorporates several structural differences, including stiffer wings than the block 25 F-16. Examination of analytical mode shapes shows that the basic flutter mechanisms of a block 40 and a block 25 aircraft are similar. In addition, flutter flight-test data confirm that the aeroelastic instabilities are similar between block 25 and block 40 F-16 aircraft. Flight-test results of aeroelastically sensitive configurations have shown LCO onset speed and magnitude can vary between the block 25 and block 40 versions of the F-16; however, LCO is typically present for both.

The F-16 has nine primary stations upon which to carry external stores. Extra fuel can be carried in external tanks under the wings (stations 4 and 6) and the fuselage (station 5). Air-to-air missiles are typically carried on the two outboard stations of each wing (stations 1, 2, 8, and 9). The remaining two wing hardpoints (stations 3 and 7) typically carry air-to-ground stores. The aircraft used for these tests were modified for flutter testing. These modifications make it uniquely capable of sensing, recording, and transmitting data gathered during tests. Figure 1 shows the location of accelerometers that are monitored and measured on these flight tests. The F-16 flutter flight-test aircraft use an onboard excitation system that is capable of sending in-phase and 180-deg out-of-phase sinusoidal signals to the flaperons. Bursts (or dwells) from 2 to 20 Hz can be selected. Sweeps that decrease uniformly from 20 to 2 Hz are also available. Both duration and amplitude are variable inputs to the flutter excitation system control panel. Flutter tests on the F-16 are typically performed with constant external fuel tank levels, that is, external fuel tanks are "locked out," disabling the ability to use that fuel.

Testing began at 10,000-ft pressure altitude (altimeter set to 29.92 in. Hg) at a low airspeed. Test points increasing in airspeed are completed at that altitude before proceeding to another altitude. At each test point, flaperon bursts and sweeps were performed at the discretion of the lead flutter engineer. Elevated load factor turns were also performed to determine the sensitivity of the aeroelastic instability to the change in angle of attack and trim conditions. A test-point maneuver was terminated when the response amplitude either exceeded predetermined termination criteria or the response amplitude increased at such a rate as to rapidly approach the predetermined termination criteria. A complete overview of Eglin Air Force Base F-16 flutter testing can be found in Ref. 12. Additionally, F-16 test instrumentation and flight-test methods are described more thoroughly in Ref. 5.

Table 1 Flight-test configurations

	Left wing					Right wing			
Configuration	Station 1	Station 2	Station 3	Station 4	Station 5	Station 6	Station 7	Station 8	Station 9
				Set I					
1 (Asym)	AIM-9	AIM-9	AGM-65	370 Tk (FFF)	——	370 Tk (FFF)	AGM-88	AIM-9	Lau
2 (Sym)	Lau	AIM-9	AGM-88	370 Tk (FEE)	——	370 Tk (FEE)	AGM-88	AIM-9	Lau
3 (Sym)	AIM-9	AIM-9	AGM-65	370 Tk (FFF)	——	370 Tk (FFF)	AGM-65	AIM-9	AIM-9
				Set II					
4 (Asym)	Lau	AIM-9	AGM-65	370 Tk (FEF)	——	370 Tk (FEF)	AGM-88	AIM-9	AIM-9
5 (Sym)	AIM-9	AIM-9	AGM-88	370 Tk (FEF)	——	370 Tk (FEF)	AGM-88	AIM-9	AIM-9
6 (Sym)	Lau	AIM-9	AGM-65	370 Tk (EEE)	——	370 Tk (EEE)	AGM-65	AIM-9	Lau

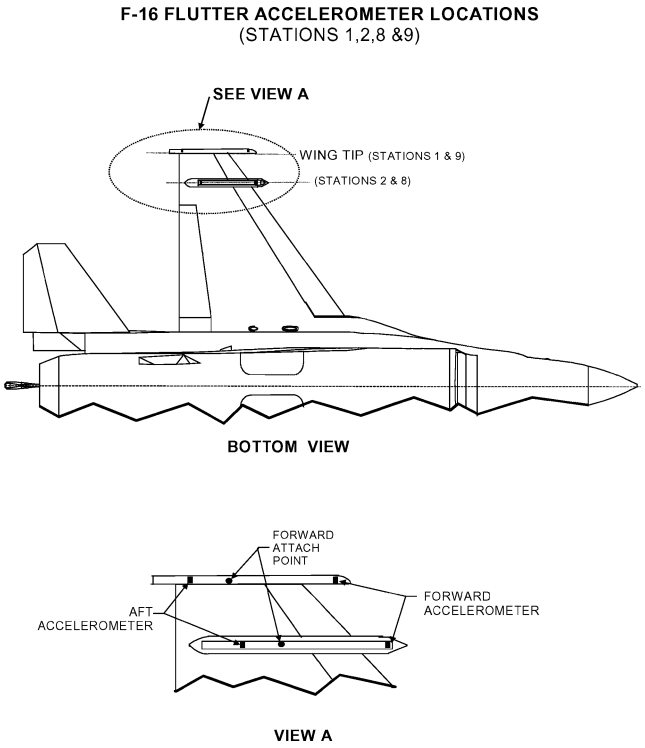

Fig. 1 F-16 accelerometer instrumentation.

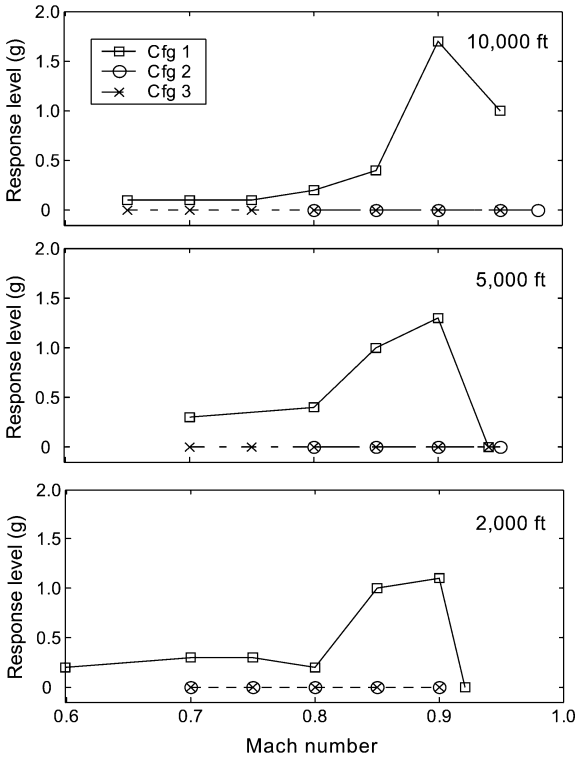

Fig. 2 Maximum measured oscillatory wing-tip response during level flight for configurations 1–3.

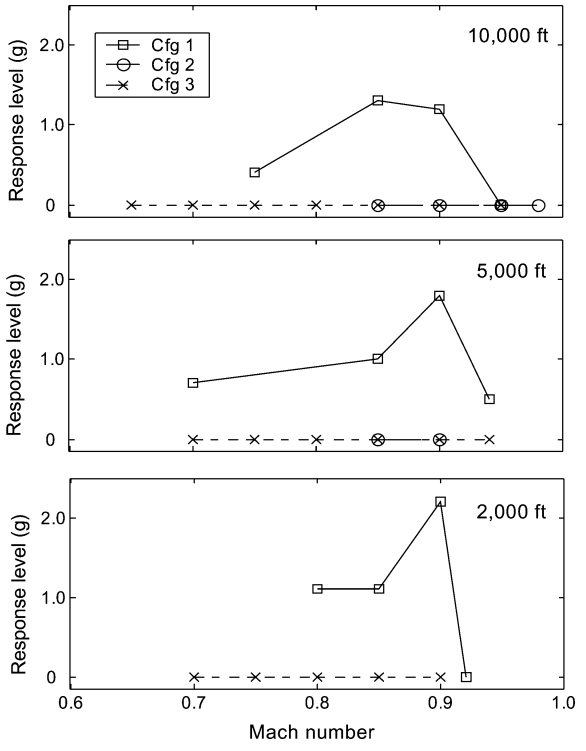

Fig. 3 Maximum measured oscillatory wing-tip response during elevated *g* for configurations 1–3.

Set I Flight-Test Results

Configuration 1 is an asymmetric configuration with the left wing identical to configuration 3 and the right wing identical to configuration 2 with the exception of the external fuel tank loading. Although the external fuel weight has an effect on the dynamic characteristics, the expense of a flight test with this weapon configuration and full external wing tanks could not be justified because of high analytical flutter speeds. The flight-test results for configuration 2 are included for completeness. Configuration 2 is a symmetric configuration with each wing carrying a single underwing AIM-9 missile, an AGM-88, and an external wing fuel tank with partial fuel. Configuration 3 is a symmetric configuration with each wing carrying two AIM-9 missiles, an AGM-65, and full external wing fuel tanks. The LCO amplitude levels measured in each of the flight tests are shown in Figs. 2 and 3. Figure 2 shows the maximum measured LCO amplitude during straight-and-level flight for configurations 1 through 3 at three altitudes: 10,000, 5000, and 2000 ft. The flight-test results during straight-and-level flight show no indication of LCO for configurations 2 and 3; the asymmetric combination, however, demonstrates low-level LCO starting as early as 0.6 Mach at 2000 ft. The oscillations grow in magnitude with increasing dynamic pressure and Mach number. The maximum LCO response for configuration 1 is encountered at 0.9 Mach, after which it starts to diminish. Figure 3 shows the maximum measured LCO amplitude during elevated *g* maneuvers. Again, flight-test results show no aeroelastic instability for symmetrical configurations 2 and 3 at any flight-test altitude. Configuration 1 is shown to have higher LCO levels at elevated *g* than during straight-and-level flight; however, the LCO response follows the same trend of peaking at approximately 0.9 Mach. The oscillatory response for configuration 1 occurs at 5.5 Hz.

Figure 4 shows wing-tip accelerometer response data at test conditions of 5000 ft/0.90 Mach during straight-and-level flight. An 11-Hz low-pass filter is applied to this flight-test data. The top plot in Fig. 4 is an overlay of the left wing forward (1FV) and the right wing forward (9FV) vertical accelerometer response. The forward accelerometers show similar amplitude response levels for the left and right wing and are approximately 180 deg out of phase, indicating an antisymmetric-type response. The bottom plot shows the left-wing-aft (1AV) and the right-wing-aft (9AV) vertical accelerometer response overlaid. The right-wing-forward accelerometer slightly leads the right wing aft accelerometer, and has similar response levels. The left-wing-aft accelerometer is not a clean 5.5-Hz sinusoidal signal, however some content at minimal response levels is shown. From the accelerometer response data, it can be seen that the right wing is mostly bending motion, and the left wing is mostly outboard wing torsion, with the torsion node line running near the aft accelerometer.

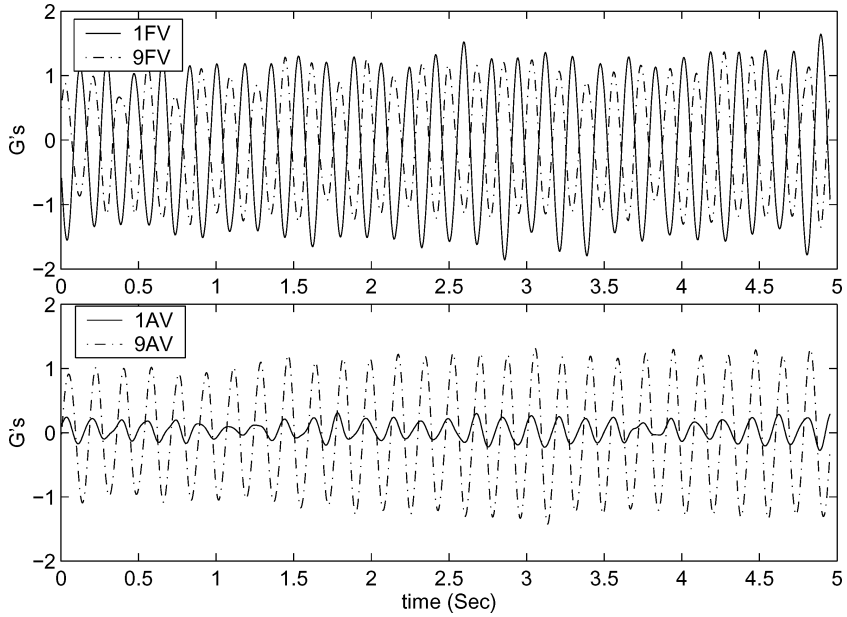

Fig. 4 Configuration 1: wing-tip accelerometer response at 0.9 Mach, 5000 ft.

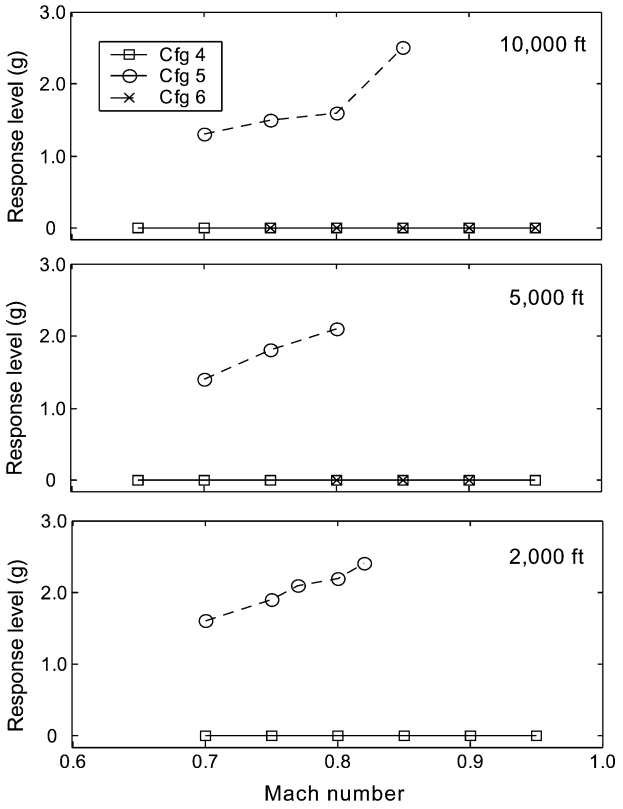

Fig. 5 Maximum measured oscillatory wing-tip response during level flight for configurations 4–6.

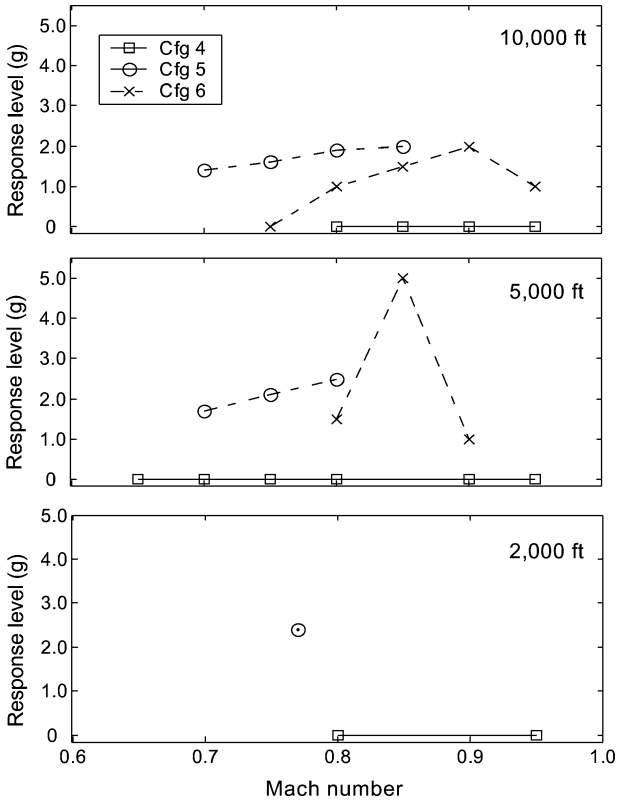

Fig. 6 Maximum measured oscillatory wing-tip response during elevated *g* for configurations 4–6.

Set II Flight-Test Results

Configuration 4 is an asymmetric configuration with the right wing identical to configuration 5 and the left wing similar to configuration 6 with the exception of the external fuel tank loading. Configuration 5 is a symmetrically loaded configuration with each wing carrying two AIM-9 missiles, an AGM-88, and a partially filled external wing fuel tank. Configuration 6 is a symmetrically loaded configuration with each wing carrying a single AIM-9 missile underwing, an AGM-65, and an empty external wing fuel tank. Figures 5 and 6 show the LCO response for configurations 4 through 6 for straight-and-level flight and during elevated g. Only configuration 5 shows LCO during straight-and-level flight. LCO amplitudes greater than 1 g were found at 0.7 Mach at all altitudes and increased with Mach and dynamic pressure until the predetermined limit was exceeded. During elevated g maneuvers, significant levels of LCO are shown for configuration 6 at both 5000 ft and 10,000 ft. At 0.85 Mach, 5000 ft, the LCO levels for configuration 6 jumped to 5 g. The LCO response level for configuration 5 remained nearly constant between straight-and-level flight and during elevated g flight. No LCO response was detected for the asymmetric

combination of these two symmetric configurations, as indicated in Figs. 5 and 6.

Analysis Results

Two structural models were used in the original linear flutter analysis when the flight-test program was developed. A half-span FEM model was used for the symmetrically loaded configurations, applying symmetric and antisymmetric boundary conditions. A full-span FEM that is the equivalent of two half-span models joined at the centerline was created. The full-span FEM was validated by comparing the eigenvalues and flutter speeds of a symmetrically loaded configuration to the half-span results for both symmetric and antisymmetric boundary conditions. The flutter speeds and mode shapes shown in this paper are all generated from a full-span FEM, although the results for a symmetrically loaded configuration are identical to the half-span model results. The full-span structural model includes a flexible wing, control surfaces, fuselage, and horizontal and vertical tails. The full-span aerodynamic model incorporates all lifting surfaces and is divided into 15 panels, three for the vertical tail and rudder, two for the horizontal tails, eight for the wings, and two for the fuselage. There are a total of 616 boxes for the full aircraft aerodynamic model. External stores were not aerodynamically modeled to facilitate the large number of analyses typically required for external store certification. Experience with the numerous F-16 flight-tested configurations has shown that good correlation of flutter analyses have been obtained without the store aerodynamics. NASTRAN was used to perform the analysis, using the Lanczos method to obtain the vibration solution, and the KE method to obtain the flutter solution. The doublet-lattice method was used to generate subsonic unsteady aerodynamic forces, while a constant pressure method was used to generate the supersonic unsteady aerodynamic forces.

The calculated flutter speed at 0.9 and 1.2 Mach are listed for configurations 1 through 6 in Table 2. Recall that symmetric configurations 2 and 6 had partial and empty external fuel loadings, while their corresponding wings on the asymmetric configurations had full external fuel tanks. The flutter speeds for the exact fuel loading as flown on the asymmetric configuration are shown as configurations 2a and 6a. During the external store certification process, only the flutter speeds at 0.9 and 1.2 Mach are typically examined to determine the aeroelastic critical mode.

Set I Analysis Results

The flutter speeds in Table 2 show that both symmetrically loaded configurations 2a and 3 predict high flutter speeds. The asymmetric combination, however, has low flutter speeds of 513 kn at 0.9 Mach and 483 kn at 1.2 Mach. The matched point flutter solution was generated for configurations 1, 2a, and 3, and is shown in Fig. 7. Although the matched point flutter solution for configuration 3 dips at 1.05 Mach, it cannot be inferred from the half-span results that the flutter speeds of the asymmetric combination will be lower than either of the symmetrically loaded configurations. Table 3 shows the natural frequencies of the primary modes for each configuration. The mode shapes of the critical flutter mechanism for configuration 1 are shown in Figs. 8 and 9. It is clear that the outboard wing torsion mode

Table 2 Flutter speeds at $g = 0.02$, sea level

			$M = 0.90$		$M = 1.20$	
Configuration	Model	Fuel tank	V_f KEAS	f_f, Hz	V_f KEAS	f_f, Hz
		Set I				
1	Blk 25	(FFF)	513	5.5	483	5.6
2	Blk 40	(FEE)	945	7.0	793	6.9
2a	Blk 25	(FFF)	921	6.3	782	6.2
3	Blk 25	(FFF)	716	4.9	No crossing	
		Set II				
4	Blk 25	(FEF)	922	5.8	971	7.0
5	Blk 25	(FEF)	434	5.2	No crossing	
6	Blk 25	(EEE)	614	8.0	494	8.1
6a	Blk 25	(FEF)	929	6.9	775	6.9

Table 3 Frequencies and mode-shape descriptions

f_n	Mode shape
	Configuration 1
4.06	Wing bending (sym)
5.37	AGM-88 store lateral (anti W1B)
5.53	AGM-65 tip Missile Pitch (sym)
5.80	AGM 65 tip Missile Pitch (anti)
6.98	External fuel tank lateral (sym)
	Configuration 2a
4.46	Sym wing bending
5.35	Anti AGM-88 store lateral
5.64	Sym AGM-88 store pitch
6.96	Sym external fuel tank lateral
	Configuration 3
3.83	Sym wing bending
5.08	Anti W1B
5.47	Anti AGM-65 pitch
5.60	Sym store pitch
6.13	Sym tip missile pitch
7.11	Sym tank lateral

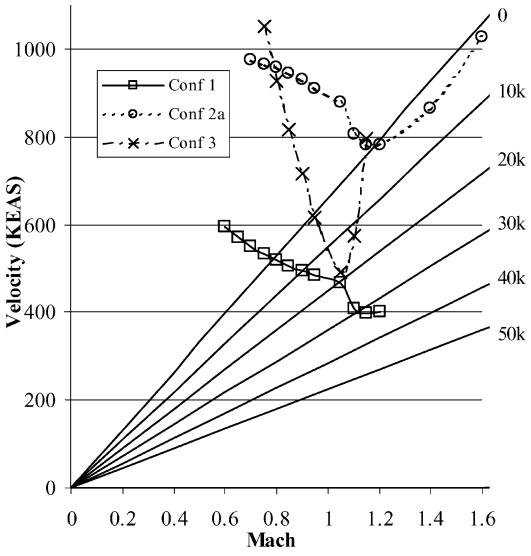

Fig. 7 Matched point flutter solution for configurations 1, 2a, and 3.

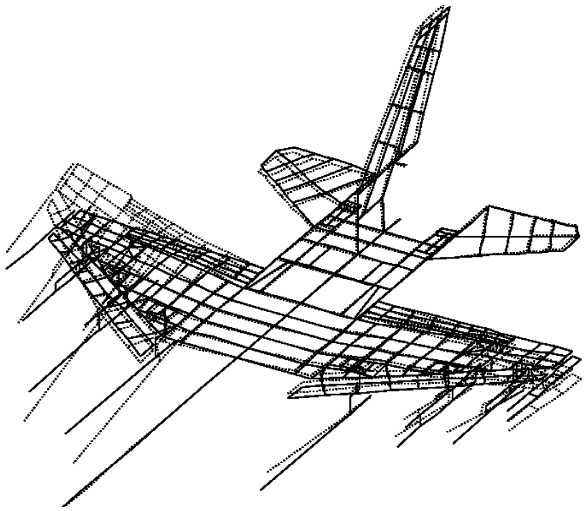

Fig. 8 Configuration 1: right-wing bending, asymmetric coupling mode, $f = 5.37$ Hz.

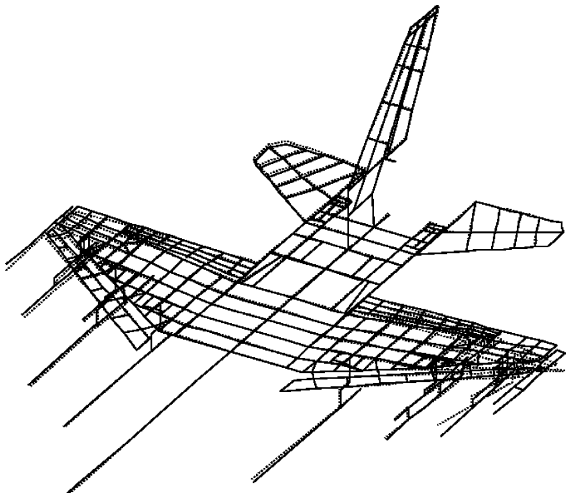

Fig. 9 Configuration 1: left-wing outboard wing torsion, $f = 5.53$ Hz.

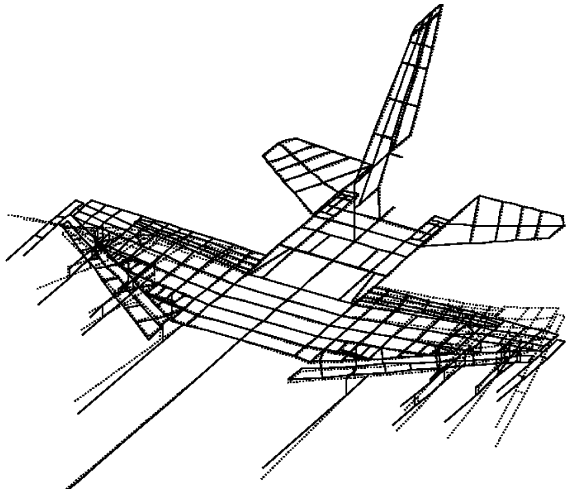

Fig. 10 Configuration 3: antisymmetric AGM-65 pitch, $f = 5.47$ Hz.

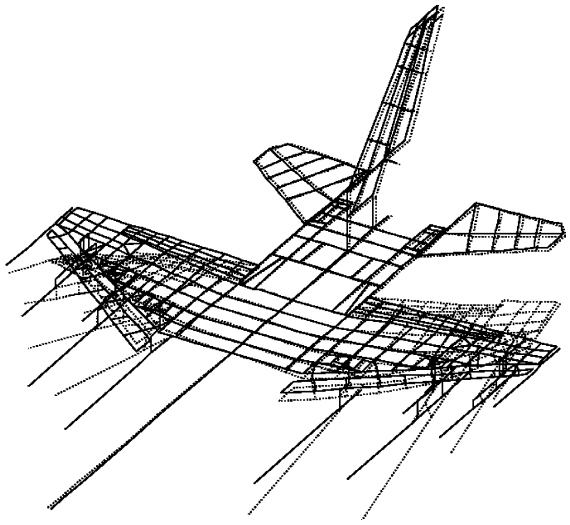

Fig. 11 Configuration 2a: antisymmetric wing bending, $f = 5.35$ Hz.

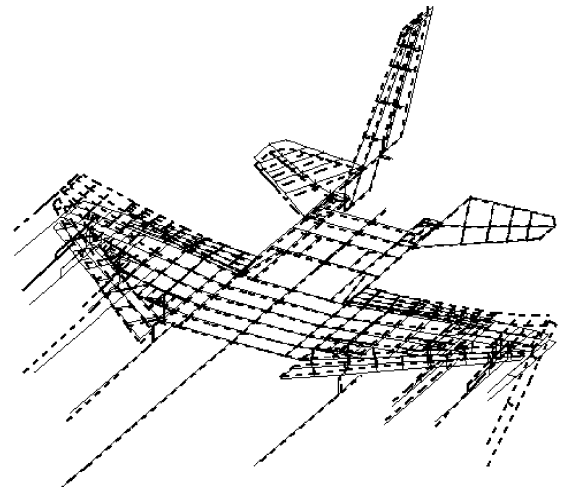

Fig. 12 Configuration 1: flutter eigenvector $M = 0.9$, $V = 430$ KTAS, alt = 0 ft.

caused by the AGM-65 store pitch (left wing) of configuration 1 in Fig. 9 can be associated with the same antisymmetric outboard wing torsion mode of the symmetrically loaded configuration 2 in Fig. 10. The frequencies are similar, 5.53 Hz vs 5.47 Hz. Similarly, the right wing bending mode in Fig. 8 is associated with the same antisymmetric wing bending mode of symmetrically loaded configuration 2a shown in Fig. 11. Again, the frequencies are similar, 5.37 Hz vs 5.35 Hz. The mechanism for configuration 1 appears to be a pure asymmetric mechanism, one that is not predictable with interpretation of half-span analyses.

An important observation is that the asymmetric modes that couple as demonstrated in flight test are essentially the antisymmetric equivalent of the modes of the symmetrically loaded configurations. This follows the trend that LCO on the F-16 is predominantly an antisymmetric phenomenon. Denegri in Ref. 5 states that antisymmetric LCO might be dominant because a more viable side-to-side energy transfer path exists through the aircraft rolling motion than through the fuselage pitch and plunge motions. Referring back to Fig. 5, the strip chart data show an antisymmetric response between the forward wing-tip accelerometers. The flutter eigenvector was generated using 0.9 Mach aerodynamics at 430 kn with a sea-level density ratio. Figure 12 shows the flutter mode shape. Comparison of this flutter mode shape to the wing-tip accelerometer response in Fig. 5 shows good correlation. Nearly in-phase and equal amplitude motion is shown on the right wing. The left wing shows more forward wing-tip response and minimal response at the location of the aft-wing accelerometer. The left wing-tip phase difference from Fig. 5 shows that the node line runs near the aft accelerometer, as shown in Fig. 12.

Set II Analysis Results

The flutter speeds in Table 2 show that both symmetrically loaded configurations 5 and 6 predict low flutter speeds, a prediction that was validated with the flight-test results. The asymmetric combination of these two loadings is predicted to have high flutter speeds at 0.9 and 1.2 Mach. The matched point flutter solution was generated for configurations 4, 5, 6, and 6a, and is shown in Fig. 13. Table 4 shows the natural frequencies of the primary modes of the asymmetric configuration and the corresponding frequencies of each half when symmetrically loaded. The mode shapes of the critical flutter mechanism for configuration 5 are shown in Figs. 14 and 15. The coupling flutter mode shapes for configuration 4 are shown in Figs. 16 and 17. The aft-wing bending in Fig. 14 is seen on the right wing of the asymmetric configuration in Fig. 17. The AGM-88 pitch in Fig. 15 at 5.30 Hz is also seen on the right wing of the asymmetric mode shape in Fig. 16 at 5.36 Hz. The AGM-88 store pitch for the symmetrically loaded configuration has a natural frequency of 5.29 Hz, while the corresponding AGM-88 store pitch frequency for the asymmetric configuration is 5.79 Hz. Table 4 shows that the coupling modes of configuration 5 have swapped position and have separated in frequency. The increase in flutter speed for the asymmetric configuration could therefore be explained as a detuning of the critical modes.

Table 4 Frequencies and mode-shape descriptions

f_n	Mode shape
	Configuration 4
4.13	W1B (sym)
5.36	AGM-88 store pitch
5.79	Aft-wing bending on AGM-88 wing
6.55	AGM-65 store pitch
7.70	AGM-88 store lateral
7.87	External fuel tank lateral (sym)
	Configuration 5
3.83	Sym wing bending
5.29	Antoutboard wing bending
5.30	Anti AGM-88 store pitch
5.42	Sym AGM-88 store pitch
6.34	Sym AGM-88 store lateral
7.67	Anti AGM-88 store lateral
7.87	Sym external fuel tank lateral
	Configuration 6a
4.71	Sym W1B
6.26	Anti AGM-65 pitch
6.70	Sym AGM-65 pitch
7.87	Anti aft-wing bending
7.87	Sym external fuel tank lateral
7.11	Sym tank lateral

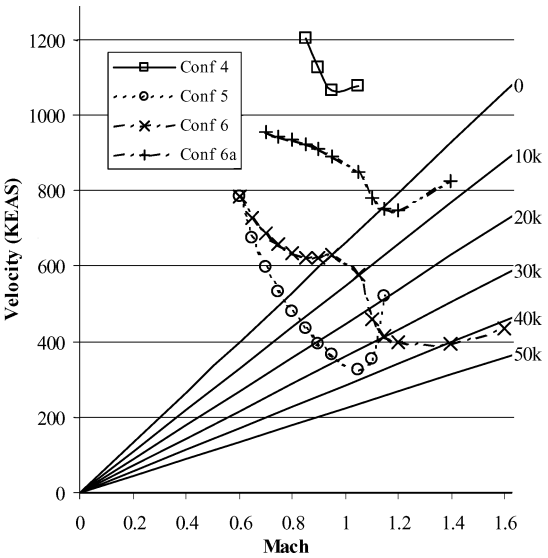

Fig. 13 Matched point flutter solution for configurations 4, 5, 6, and 6a.

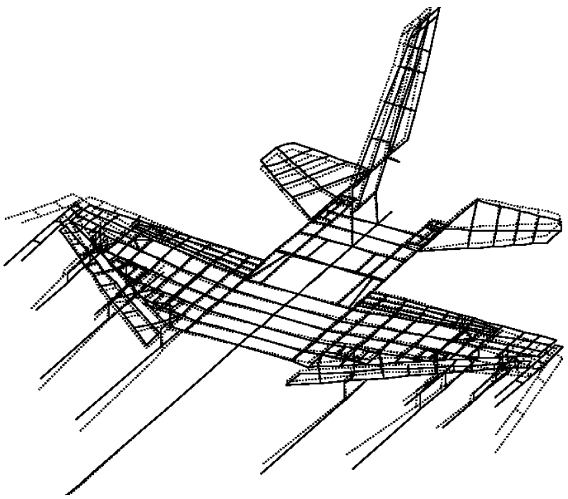

Fig. 14 Configuration 5: antisymmetric aft-wing bending, $f = 5.29$ Hz.

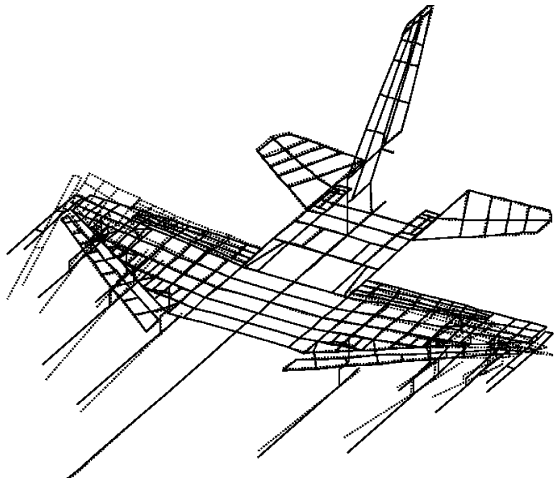

Fig. 15 Configuration 5: antisymmetric AGM-88 pitch, $f = 5.30$ Hz.

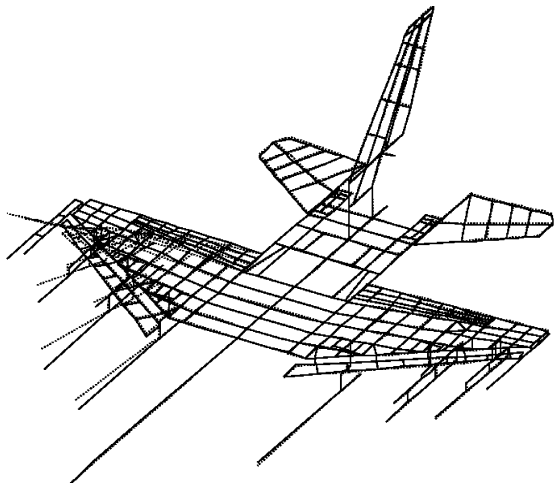

Fig. 16 Configuration 4: AGM-88 pitch, $f = 5.36$ Hz.

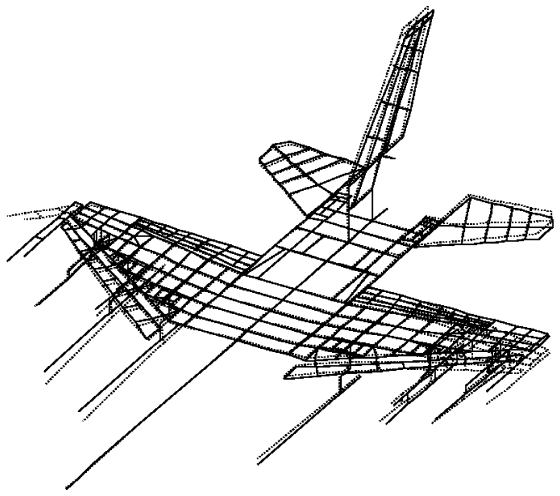

Fig. 17 Configuration 4: wing bending, $f = 5.79$ Hz.

Conclusions

Flutter analysis and flight testing of asymmetric external store configurations on an F-16 were conducted. These results were compared to the flutter analysis and flight-test results of the symmetric external store loading of each wing of the asymmetric configuration, that is, for an asymmetric configuration XY, analyses and flight tests of the configurations XX and YY were performed. It has been shown that asymmetric configurations can have either higher or lower analytical flutter speeds than the corresponding symmetric configuration. In addition, it was also shown that limit-cycle oscillations can

occur at either higher or lower airspeeds or dynamic pressures (or not at all) with varying response amplitudes than the corresponding symmetric configurations. Although the flutter mechanism for the asymmetric configurations involves the coupling of asymmetric modes, these modes can be traced to similar antisymmetric modes of each wing of the symmetric models by examination of the mode shapes. Even when analyzing full-span asymmetric configurations, the half-span concepts of symmetric and antisymmetric motion still play a part in understanding the aeroelastic response. One explanation for the variation in the onset speeds of limit-cycle oscillation is that the coupling modes of the unstable wing have become tuned or detuned. It was also shown that asymmetric modes with origins in symmetric and antisymmetric modes are now coupling, creating a purely asymmetric aeroelastic unstable mechanism.

It was determined that the use of half-span models for certification of external store downloads is not a reliable technique for recent asymmetric store configurations. It can lead to an unnecessary reduction in aircraft capability, or, much worse, a critical flutter condition can go undetected until discovered, possibly catastrophically, in the field. Historically, the use of half-span models was a necessity because of computational limitations. Recent technological advances are removing these limitations, however, and allowing those involved in certification to provide maximum capability without compromising safety.

References

[1]Bunton, R. W., and Denegri, C. M., Jr., "Limit Cycle Oscillation Characteristics of Fighter Aircraft," *Journal of Aircraft*, Vol. 37, No. 5, 2000, pp. 916–918.

[2]Cunningham, A. M., Jr., and Meijer, J. J., "Semi-Empirical Unsteady Aerodynamics for Modeling Aircraft Limit Cycle Oscillations and Other Non-Linear Aeroelastic Problems," *Proceedings of the International Forum on Aeroelasticity and Structural Dynamics*, Vol. 2, Royal Aeronautical Society, London, 1995, pp. 74.1–74.14.

[3]Meijer, J. J., and Cunningham, A. M., Jr., "A Semi-Empirical Unsteady Nonlinear Aerodynamic Model to Predict Transonic LCO Characteristics of Fighter Aircraft," AIAA Paper 95-1340, April 1995.

[4]Chen, P. C., Sarhaddi, D., and Liu, D. D., "Limit-Cycle Oscillation Studies of a Fighter with External Stores," AIAA Paper 98-1727, April 1998.

[5]Denegri, C. M., Jr., "Limit Cycle Oscillation Flight Test Results of a Figher with External Stores," *Journal of Aircraft*, Vol. 37, No. 5, 2000, pp. 761–769.

[6]Katz, H., "Flutter of Aircraft with External Stores," *U.S. Air Force Aircraft/Stores Compatibility Symposium*, McDonnell Aircraft Co., St. Louis, MO, 1969, pp. 1–15.

[7]Sensburg, O., Lotze, A., and Haidl, G., "Wing with Stores Flutter on Variable Sweep Wing Aircraft," *AGARD Conference Proceedings*, No. 162, NATO, Neuilly Sur Seine, France, 1974, pp. 6.1–6.19.

[8]Lotze, A., "Asymmetric Store Flutter," AGARD, Rept. 668, NATO, Neuilly Sur Seine, France, April 1978, pp. 1–20.

[9]Maricic, N. L., "Calculation of Critical Flutter Speeds of an Aircraft in Subsonic Flow," *Computers and Structures*, Vol. 12, Oct. 1980, pp. 475–482.

[10]Guruswamy, G. P., and Tu, E. L., "Effects of Symmetric and Asymmetric Modes on Transonic Aeroelastic Characteristics of Full-Span Wing-Body Configurations," AIAA Paper 88-2308, April 1988.

[11]Dawson, K. S., and Sussingham, J. C., "F-16 Limit Cycle Oscillation Testing with Asymmetric Stores," AIAA Paper 99-3142, June 1999.

[12]Dreyer, C. A., and Shoch, D. L., "F-16 Flutter Testing at Eglin Air Force Base," AIAA Paper 86-9819, April 1986.